Earth and Planetary Science Letters 304 (2011) 503–510

Contents lists available at ScienceDirect

Earth and Planetary Science Letters

journal homepage: www.elsevier.com/locate/epsl

Monsoon speeds up Indian plate motion

Giampiero Iaffaldano [a,*], Laurent Husson [b,c], Hans-Peter Bunge [d]

[a] Research School of Earth Sciences, The Australian National University, Australia
[b] CNRS UMR6118, Géosciences Rennes, France
[c] CNRS UMR 6112, Laboratoire de Planétologie et Géodynamique de Nantes, France
[d] Department of Earth and Environmental Sciences, LMU Munich, Germany

ARTICLE INFO

Article history:
Received 8 November 2010
Received in revised form 10 February 2011
Accepted 14 February 2011

Editor: Y. Ricard

Keywords:
Indian monsoon
Himalayan erosion
topography evolution
Indian plate-motion change

ABSTRACT

Short-term plate motion variations on the order of a few Myr are a powerful probe into the nature of plate boundary forces, as mantle-related buoyancies evolve on longer time-scales. New reconstructions of the ocean-floor spreading record reveal an increasing number of such variations, but the dynamic mechanisms producing them are still unclear. Here we show quantitatively that climate changes may impact the short-term evolution of plate motion by linking explicitly the observed counter-clockwise rotation of the Indian plate since ~10 Ma to increased erosion and reduced elevation along the eastern Himalayas, due to temporal variations in monsoon intensity. By assimilating observations into empirical relations for the competing contributions of erosion and mountain building, we estimate the first-order decrease in elevation along the eastern Himalayas since initial strengthening of the monsoon. Furthermore, we show with global geodynamic models of the coupled mantle/lithosphere system that the inferred reduction in elevation is consistent with the Indian plate motion record over the same period of time, and that lowered gravitational potential energy in the eastern Himalayas following stronger erosion is a key factor to foster plate convergence in this region. Our study implicates lateral variations in plate coupling and their temporal changes as an efficient source to induce an uncommon form of plate motion where the Euler pole falls within its associated plate.

1. Introduction

A prominent feature of the Himalayan morphology is the along-arc profile of its relief. Elevation gently increases eastward from an average of 3 km in Kashmir and Ladakh towards the summits of Nepal where most of the world's highest peaks reach altitudes of more than 6 km, and decreases back to a mean value of 2 km further east. The Himalayas is also home to significant rainfall gradients. Observations of annual precipitation (Pidwirny, 2006) yield an increase from about 1 to 4 m as one moves eastward along the belt (Fig. 1A). A spectral analysis of the precipitation profile (Fig. 1B) indicates that contributions from wavelengths longer than 1000 km constitute the bulk of rainfall variations along the entire belt (Fig. 1A — dashed line).

At present-day, the Indian monsoon results in abundant rainfall along the eastern Himalayas. It has been speculated that the monsoon intensified between 9 and 6 Ma, when the Tibetan plateau attained sufficient elevation to act as a heat source and to block northward air fluxes (Molnar et al., 1993). Results of atmospheric circulation modelling, however, suggest that the Himalayan front by itself may suffice to act as an orographic barrier and drive monsoonal activity (Boos and Kuang, 2010), potentially pushing the onset of monsoon intensification sometime into the mid-Miocene (Ramstein et al., 1997). The paleobotanical record of western India indeed agrees with this view. In fact, tropical species typical of a wet climate progressively made their appearance during this period, as opposed to earlier times that were characterised by the presence of dryer-climate plants (Travese, 1982; Wolfe, 1985).

While these results indicate important interplays between orogeny, erosion and climate, the sedimentary record from stratigraphic field-collections and ocean-floor drillings (Garzione et al., 2003) bears a more complex relationship. An et al. (2001) analysed aeolian and marine sediments to place the onset of strong monsoonal activity between 12 and 8 Ma, followed by a period of constant intensity that persisted at least until the end of the Pliocene. On the other hand Le Treut et al. (1994) detected a mid-Miocene increase in the sedimentation rates of the Bengal fan, which samples the Himalayas since at least the early Miocene (Ramstein et al., 1997), and interpreted this as evidence of intensification. More recently, Clift et al. (2008) argued for a non-monotonic evolution of monsoon intensity and erosion in the Himalayas by analysing the chemistry and mineralogy of sediments transported into the Bengal fan, Arabian Sea, and South China Sea. This record shows a maximum of erosion from 15 to 10 Ma, which decreases progressively until the beginning of the Pleistocene, before returning to its present-day value (Fig. 2). Regardless of when intensification precisely started, the sedimentary

* Corresponding author at: Research School of Earth Sciences, The Australian National University, Bldg 61 Mills Road, Acton, ACT 2601, Australia. Tel.: +61 2 612 53424 (Office).
E-mail address: giampiero.iaffaldano@anu.edu.au (G. Iaffaldano).

0012-821X/$ – see front matter © 2011 Elsevier B.V. All rights reserved.
doi:10.1016/j.epsl.2011.02.026

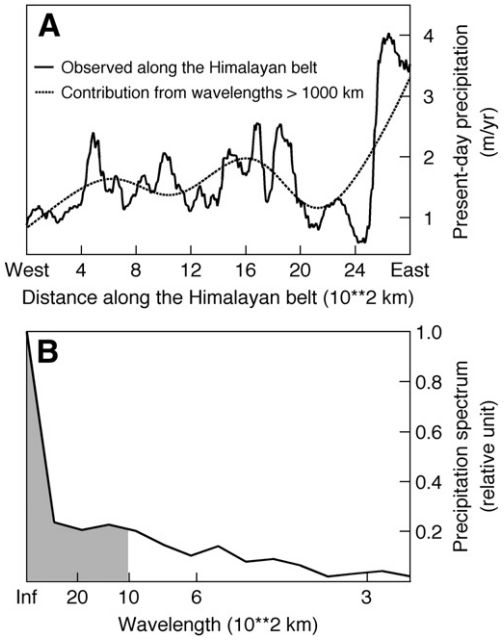

Fig. 1. (A) Precipitation intensity (solid line) observed within the Himalayan belt. At any distance, we report the average value observed along a track cutting into the Himalayas parallel to the direction of India/Eurasia convergence. Precipitation increases from 1 to 4 m/yr from west to east. The dashed line is the precipitation pattern resulting from contributions of wavelengths longer than 1000 km. (B) Spectrum of present-day precipitation intensity. Note that wavelengths longer that 1000 km (grey area) constitutes the bulk of precipitation along the Himalayan belt.

record provides ample evidence that the Indian monsoon efficiently erodes the eastern Himalayas. It is therefore reasonable to assume that monsoon intensification and stronger erosion contributed to shape the peculiar topographic profile we observe today along the Himalayan front, particularly along the eastern end.

The geomorphologic evolution of the Himalayas has, of course, implications for the dynamics of the India/Eurasia convergent system, because the gravitational potential energy stored in the thick crust of mountain belts yields forces comparable to other driving and resisting forces available in plate tectonics (Ghosh et al., 2006; Husson and Ricard, 2004; Iaffaldano et al., 2006). Large orogens are capable of deforming the interior of plates, as for instance in the Indian Ocean following the rise of the Tibetan plateau (Bull and Scrutton, 1990), or to modify the rate of convergence between overriding and subducting plates (Iaffaldano and Bunge, 2009). Likewise, the recent episode of plateau formation in the Andes decreased the convergence rate between the Nazca and South American plates substantially, and had a profound effect on plate motion in the broader Pacific and Atlantic Oceans (Husson et al., 2008; Iaffaldano et al., 2007). In this study we

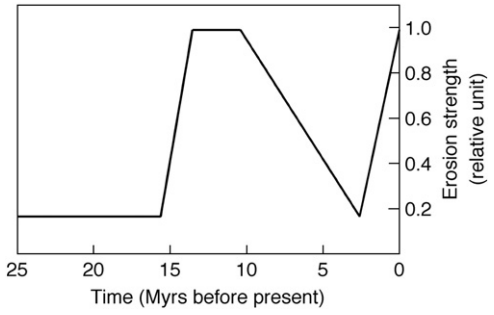

Fig. 2. Variations of erosion strength since 25 Ma relative to present-day, constrained by chemical and mineralogical indicators from sediments transported into the Bengal fan, Arabian Sea, and South China Sea. Observations indicate two periods of peak erosion, from 15 to 10 Ma, as at the present-day (see Section 1 for details and references).

test the hypothesis that a link exists between the monsoon-shaped geomorphology of the Himalayas since mid-Miocene and the history of India/Eurasia plate convergence.

2. Reconstruction of India/Eurasia relative motion since magnetic anomaly 5An.2o (~12.4 Ma)

2.1. General setting

The long-lasting convergence between the Indian and Eurasian plates evolved into a collision when the Tethys Ocean closed, and the Indian continental crust approached the subduction system around 50 Ma (Chemenda et al., 2000; Patriat and Achache, 1984). This event is regarded as the prelude to the overall reduction of the convergence from ~20 cm/yr to ~4 cm/yr (Copley et al., 2010). Until Miocene, India was part of the Indo-Australian plate. While the details of the eventual dismantling of this large plate are debated (Conder and Forsyth, 2001; DeMets et al., 2005; Gordon et al., 2008; Royer and Gordon, 1997; Wiens et al., 1985), it is thought that the Indo-Australian plate at present-day is divided into the Macquarie, Australian, Capricorn, and Indian plates. Separation of the latter might have initiated as early as 18 Ma. But only around 10 Ma did India behave as an individual plate, and the relative motion of plates in the Indian Ocean realm become steady (Gordon et al., 1998; Merkouriev and DeMets, 2006). On its southwestern side India separated from Africa due to spreading of the Carlsberg ridge. The event was followed by the split of Africa into the two sub-plates of Nubia and Somalia (DeMets et al., 2005) along the East African Rift, which initiated in early Miocene (Pik et al., 2008) and must be taken into account when estimating the recent India/Eurasia convergence.

Here we take advantage of a selection of published finite rotations (Horner-Johnson et al., 2007; Merkouriev and DeMets, 2006, 2008; Mueller et al., 1999) to map the convergent motion history of India towards Eurasia since anomaly 5An.2o, which corresponds to 12.415 Ma according to the geomagnetic timescale of Lourens et al. (2004). Specifically, we solve for the India–Somalia–Nubia–North America–Eurasia plate circuit to compute Euler poles for the motion of India relative to Eurasia during four stages between 5An.2o (12.415 Ma), 5n.1y (9.779 Ma), 3An.2o (6.733 Ma), 2An.3o (3.596 Ma), and the present-day. Note that while one must interpolate the available records of Somalia–Nubia and Nubia–North America relative motions into these stages, the finite rotations for India–Somalia and North America–Eurasia relative motions published by Merkouriev and DeMets (2006, 2008) are available at a higher temporal resolution that includes the above mentioned anomalies. However, some of them carry significant variances, particularly the older ones. Typically, one subtracts any two finite rotations of one plate with respect to another to compute the Euler pole for the relative motion during the associated stage. Inevitably this has the consequence that variances of the finite rotations add up and propagate into the uncertainty of the computed Euler pole. We therefore elect to use a selection of the finite rotations from Merkouriev and DeMets (2006, 2008) driven by the following criteria: (1) Variances of the finite rotations are relatively low, so that the resulting uncertainties on the Euler poles are kept as small as possible. (2) Selected anomalies are almost evenly spaced. (3) We avoid using anomalies 3n.1y and 4n.1y, whose edges are difficult to detect (Merkouriev and DeMets, 2006). (4) Most importantly, we ensure that all the significant changes in the relative spreading evident from the full records of India/Somalia and North America/Eurasia are preserved in our selection of anomalies (see supplementary material).

2.2. India–Somalia relative spreading

We reconstruct the sequence of Euler poles for the spreading of India relative to Somalia at the above mentioned stages from the data

of Merkouriev and DeMets (2006), who show that the overall spreading rate decreased from ~4.2 cm/yr to ~3 cm/yr between 20 and 10 Ma, and remained stable ever since. Note that our selection of finite rotations for this portion of the plate circuit preserves the spreading rate decrease (see supplementary material).

2.3. Somalia–Nubia relative spreading

The kinematics of rifting between Nubia and Somalia since ~3.16 Ma is well constrained by the study of Horner-Johnson et al. (2007), who identified anomaly 2An.2n along the South West Indian Ridge and the Andrew Bain Transform Fault. Geodetic measurements of present-day displacement along the East African Rift (Stamps et al., 2008) yield a similar Euler pole, located offshore South Africa. It is therefore reasonable to argue that Nubia/Somalia relative motion remained stable over the past ~3 Myr. The relative motion at earlier ages is available from the studies of Lemaux et al. (2002) and Royer et al. (2006). However, at odds with the well-established recent kinematics, the study of Lemaux et al. (2002) locates the rotation pole along the Brazilian coastline, implying an unusual history of motion since ~11 Ma across the East African Rift, as pointed out by Molnar and Stock (2009). Furthermore, Patriat et al. (2008) recently challenged the identification by Royer et al. (2006) of anomaly 5n.2o (~11 Ma).

Assuming that more data will become available in the future to resolve the earlier history of Nubia/Somalia relative motion, we decided to adopt a conservative approach and to assume a steady motion across the East African Rift since ~12 Ma. In our reconstruction we therefore employ the Euler pole for the Somalia/Nubia relative motion since 2An.2n (~3.16 Ma) back to 5An.2o (12.415 Ma). Our choice is not surprising if one looks at recent geological studies carried out along the East African Rift (Bonini et al., 2005; Pik et al., 2008). These studies support the notion that divergence between Nubia and Somalia began in early Miocene and find no evidence for a different spreading regime or for a stronger activity since then. The contribution of the East African Rift to the plate circuit therefore consists of translating the Carlsberg ridge and Indian plate northeastwardly.

2.4. Nubia–North America relative spreading

Mueller et al. (1999) provided finite rotations for the Nubia/North America relative motion at two stages between anomalies 6ny, 5n.1y, and the present-day. The associated Euler pole is located in the arctic region, and remained relatively stable. We use these finite rotations and interpolate the associated Euler poles into the stages bounded by 5An.2o (12.415 Ma), 5n.1y (9.779 Ma), 3An.2o (6.733 Ma), 2An.3o (3.596 Ma), and the present-day. We opted not to use the reconstruction of McQuarrie et al. (2003) for this portion of the circuit, in agreement with other recent reconstructions of India/Eurasia relative motion (e.g. Copley et al., 2010), as the study of McQuarrie et al. (2003) is based on older data from Klitgord and Schouten (1986), Srivastava and Tapscott (1986), and Srivastava et al. (1990).

2.5. North America–Eurasia relative spreading

To reconstruct the Euler pole for relative spreading in the North Atlantic we employ finite rotations from the recent study of Merkouriev and DeMets (2008). This new data reveals a previously undetected sudden decrease in spreading rates by ~20% around 7 Ma. Our selection of finite rotations for this portion of the plate circuit preserves this decrease in spreading (see supplementary material).

2.6. India–Eurasia relative motion

Table 1 in the supplementary material reports our reconstruction of the Euler poles and associated uncertainties for relative motion between the Indian and Eurasian plate. We compute uncertainties by propagating the variances of each plate-pair composing the India–Somalia–Nubia–North America–Eurasia circuit. In Fig. 3A we show the associated convergence rate history for two locations west (75°E) and east (95°E) along the India/Eurasia margin. For comparison we show the same history for the recent reconstructions of Copley et al. (2010) (Fig. 3B), and Molnar and Stock (2009) (Fig. 3C). Our reconstruction confirms a trend in the variability of the convergence rate (discussed further below, see second paragraph of this section) that was observed also by Copley et al. (2010), although they provided no error bounds. There are, however, differences when we compare our reconstruction to the one of Molnar and Stock (2009), who argue for a stable convergence of India towards Eurasia since ~12 Ma. Since we follow the same plate circuit to reconstruct the India/Eurasia relative motion, we believe that these differences arise primarily from the different Euler pole chosen to describe the Somalia/Nubia relative motion prior to ~3.16 Ma. Molnar and Stock (2009) resort to the reconstruction of Lemaux et al. (2002). But they concede that this '*almost surely is wrong*' and would imply an unusual displacement across the East African Rift (see [11] in Molnar and Stock, 2009). In our reconstruction, instead, we follow the geological studies of Bonini et al. (2005) and Pik et al. (2008), who find that rifting in Africa remained stable since at least mid-Miocene. Our reconstruction therefore assumes that Somalia/Nubia relative motion between ~12 and ~3.16 Ma equals the motion between ~3.16 Ma and the present-day, which is available from the study of Horner-Johnson et al. (2007).

The history of plate kinematics arising from our reconstruction (Fig. 3A) shows an intriguing temporal behaviour as noted above: there is a mild decrease in plate convergence between anomaly 5An.2o (12.415 Ma) and 2An.3o (3.596 Ma) following upon the more

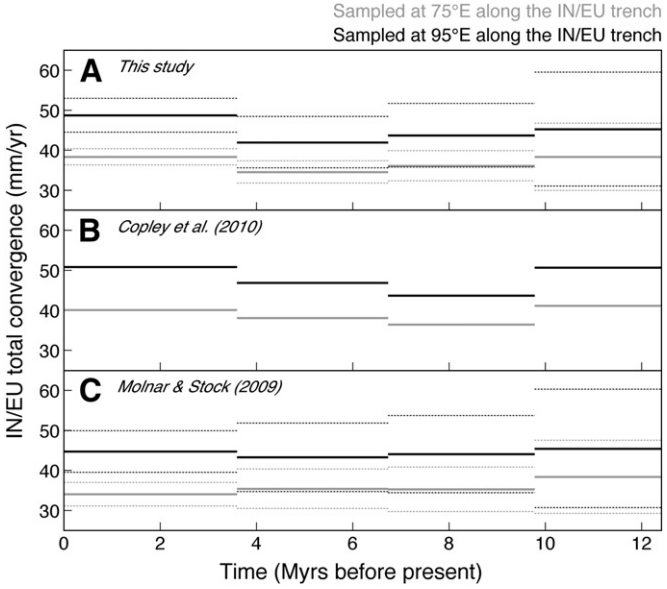

Fig. 3. (A) Reconstructed India/Eurasia total convergence (solid lines) since ~12 Ma at 95°E and 75°E along the India/Eurasia margin from this study. We compute Earth surface velocities from reconstructed Euler poles for the relative motion of India with respect to Eurasia at four stages between 5An.2o (12.415 Ma), 5n.1y (9.779 Ma), 3An.2o (6.733 Ma), 2An.3o (3.596 Ma according to the geomagnetic timescale of Lourens et al., 2004), and the present-day. Specifically, we use a selection of published finite rotations for the relative motions of India/Somlaia, Somalia/Nubia, Nubia/North America, and North America/Eurasia (see Section 2 in the main text). Note that convergence gently decreases until ~3.6 Ma, to then increase by some 5 mm/yr. Error bars (dashed lines) are computed from variances of finite rotations, following the rule of propagation of uncertainties. (B) A recent reconstruction of India/Eurasia convergence by Copley et al. (2010), interpolated within the same stages (error bars are not provided). The trend of total convergence over time is very similar to ours. (C) A recent reconstruction of India/Eurasia convergence by Molnar and Stock (2009), interpolated within the same stages. Differences with our reconstruction are more evident, and we discuss those in Section 2.6 of the main text.

pronounced slow down that occurred since ~20 Ma. This has been explained by an increase in mean elevation of the Tibetan plateau (Molnar and Stock, 2009), or alternatively by the separation of the Indian and Australian plates (Iaffaldano and Bunge, 2009). Far more interesting is the subsequent reversal of this trend, and the recent increase in convergence by more than 5 mm/yr since 2An.3o (3.596 Ma). Most importantly, the speed up is not equally partitioned between trench-normal (Fig. 4) and trench-parallel (Fig. 5) components. The trench-normal component increases during the most recent stage by some 8 mm/yr across the eastern margin, while the parallel component increases by almost the same amount along the western margin. The pattern implied by this peculiar kinematic change represents a counter-clockwise rigid rotation of the Indian plate about a pole located relatively close to – if not within – India itself. In fact, in spherical geometry as the Euler pole moves closer to a plate, one can show that the plate undergoes a more spinning motion rather than translation on the globe.

3. Models and results

There is no obvious reason for mantle related forces to evolve rapidly enough to explain this variation (Bunge et al., 1998). In fact, a recent geodynamic model (Forte et al., 2009) indicates that mantle related buoyancy forces vary only by ~1% over periods of 10 Myr or so. Similarly, by ~4 Ma the large Tibetan plateau had already attained most of its present-day elevation (Tapponnier et al., 2001). We therefore suggest that monsoon intensification induced sufficient erosion to modify the morphology of the eastern Himalayas, decreasing its elevation and crustal thickness sufficiently to affect the Indian plate motion. Specifically, we test with analytic and computational models the intriguing hypothesis that lower gravitational potential energy in the north-eastern edge of the Indian plate allowed for faster convergence across the eastern margin, thus triggering the counter-clockwise rigid rotation of the Indian plate.

It is known that significant rainfall fosters erosion in orogenic ranges, at least until one reaches a quasi steady morphological equilibrium (Beaumont et al., 1992; Willett, 1999). The characteristic time-scale of such response has been estimated to be of the order of only few Myr (Whipple and Meade, 2006). While apatite fission tracks support this notion regionally (Thiede et al., 2004), Galy and France-Lanord (2001) found at the scale of the entire Himalayas that higher erosion rates coincide with intense monsoonal rainfall. Considering that total convergence since the time of continental collision was higher in the eastern Himalayas compared to the western end (e.g. Torsvik et al., 2010), it is likely that higher erosion rates are required there to counterbalance the faster crustal influx, for otherwise elevation in the eastern Himalayas would be much higher than anywhere else along the range. Rapid exhumation of metamorphic rocks associated with stronger rainfalls (e.g. Burg et al., 1998; Finlayson et al., 2002; Thiede et al., 2004) supports such view.

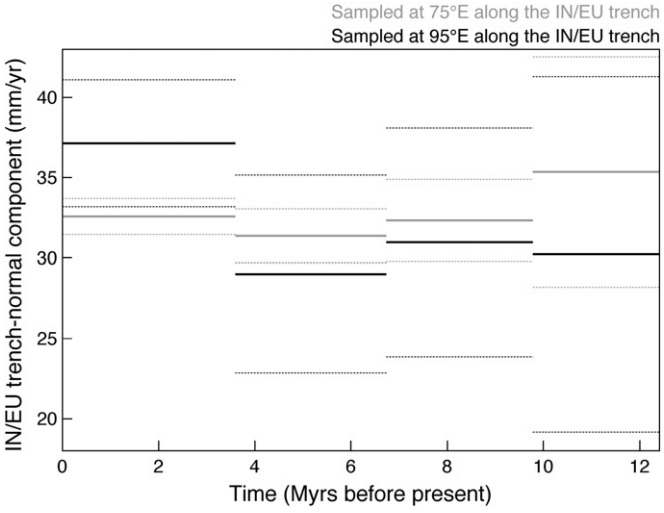

Fig. 4. Trench-normal component of the total India/Eurasia convergence, sampled at 95°E and 75°E along the India/Eurasia margin from this study. Note an increase by 8 mm/yr across the eastern margin since ~3.6 Ma. Instead, the western margin features a relatively stable trench-normal convergence.

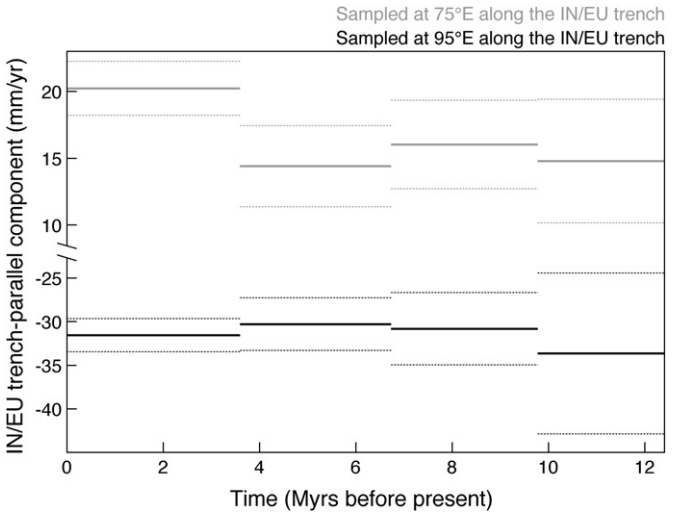

Fig. 5. Trench-parallel component of the total India/Eurasia convergence, sampled at 95°E and 75°E along the India/Eurasia margin from this study. A positive value indicates that the trench-parallel component projects westeardly along the India/Eurasia margin. A negative value indicates otherwise. Note an increase by 6 mm/yr along the western margin since ~3.6 Ma. Instead, the eastern margin features a relatively stable trench-parallel convergence. Together with the trend of the trench-normal component (see Fig. 4) the kinematic pattern reveals a counter-clockwise rigid rotation of the Indian plate about a pole located relatively close to – if not within – India itself.

3.1. Analytic model for the 2D relief of Himalayas

While estimates of paleo-elevation in the eastern Himalayas are necessarily subject to uncertainty, the present-day morphology obviously results from a dynamic equilibrium between processes responsible for mountain building, and rates at which material is eroded. The connection between rainfall and the morphology of high plateaus has been debated for a long time (e.g., Avouac and Burov, 1996; Beaumont et al., 1992; Burbank et al., 2003; Montgomery and Brandon, 2002; Whipple and Meade, 2006; Willett, 1999). Here we make no attempt to decipher the complex paths that relate them through erosion. Rather we consider the actual precipitation and morphology in the Himalayas as a result of such interplay, with insights on paleo-elevations potentially available through empirical relations between precipitation, plate convergence, and the resulting elevation (Summerfield and Hulton, 1994).

In the morphological equilibrium that shapes orogens, we regard erosion rates as a negative contribution to elevation, whereas mountain building rates are the independent, positive counterpart. We therefore set up a simple 2D analytic model to assess the time-dependent elevation of the Himalayas along the India/Eurasia margin. In our model, elevation results from the two independent contributions of mountain building rate $M(x,t)$, and erosion rate $E(x,t)$. We denote with x is the distance along the Himalayan arc, while t is the time elapsed since the collision of continental India with Eurasia at ~50 Ma. Following previous studies (Whipple and Meade, 2006), we consider the rate of mountain building to be a function of the India/Eurasia total convergence rate $V(x,t)$ in the form $M(x,t)=\beta\cdot[V(x,t)]^B$, where β and B are constants unknown *a priori* for the specific case. We constrain $V(x,t)$ from global reconstructions of plate motions (Torsvik et al., 2010). Similarly, we consider the erosion rate to be a function of the present-day precipitation $P(x)$, in the form $E(x,t)=$

$\alpha \cdot \gamma(t) \cdot [P(x)]^A$, where α and A are further constants. The term $\gamma(t)$ modulates temporal variations of the erosion strength due to intensification of the monsoon, and is provided by the reconstruction of past climate from the sedimentary record of Clift et al. (2008) (Fig. 2 — see supporting material for an alternative evolution of monsoon intensity). We obtain the precipitation at present-day along the Himalayan belt $P(x)$ from the data provided by Pidwirny (2006). In particular, we use a precipitation profile that contains only contributions from wavelengths longer that 1000 km (Fig. 1A — dashed line), computed by filtering the original precipitation data. This appears reasonable if one considers that the erosion rate in our simple model does not depend on processes occurring on regional scale, as for instance river incisions that typically enter the system of equations through the local steepness of the relief (Whipple and Meade, 2006). However, it is worth recalling that wavelengths longer than 1000 km carry the bulk of the observed rainfall along the Himalayas (Fig. 1B). Our model therefore preserves the relevant erosion pattern at the range scale. Obviously, any prediction of elevation will contain only contributions from wavelengths longer that 1000 km. Finally, as elevation along convergent margins cannot increase indefinitely, we pose at all times a limit to the elevation equal to 4200 m. This is in fact the maximum height of the observed present-day elevation, after short wavelengths have been filtered out to preserve only wavelengths longer that 1000 km.

We compute the 2D Himalayan elevation $T(x,t)$ starting at 50 Ma at time-steps $\Delta t = 1$ Myr through the following equation:

$$T(x, t + \Delta t) = \min(4200, T(x,t) + [M(x, t + {}^{\Delta t}/_{2}) - E(x, t + {}^{\Delta t}/_{2})] \cdot \Delta t). \quad (1)$$

We test our analytic model against the present-day observed elevation within the Himalayan belt. Specifically, we vary m and n in range 0 to 3 (Meade and Conrad, 2008; Whipple and Meade, 2006), while ranges for the variability of α and β are such that the time-integrated amounts of accreted and eroded material since 50 Ma across the unit length never exceed 35,000 and 20,000 m, respectively. We arrive at a set of $A = 1$, $B = 2.5$, $\alpha = 6.35 \cdot 10^{-5}\ m^{(1-A)} \cdot s^{-1}$, and $\beta = 0.14\ (m \cdot s^{-1})^{(1-B)}$ that provides the best fit to the observed elevation at present-day (Fig. 6 — solid thick lines). From this set we then compute the 2D Himalayan relief at 13 Ma, when monsoon achieves its peak strength (Fig. 6 — dashed line). The result of our analytic modelling suggests higher elevation of the eastern Himalayas in the recent past compared to present-day, possibly yielding an average altitude of ~4 km. At the same time, central and western Himalayas are predicted to be very similar to the present-day.

We tested the robustness and sensitivity of this result by taking into account a different, step-wise history of monsoon intensification, compatible with the study of An et al. (2001). Our test yields a very similar prediction of paleo-elevation at 13 Ma (see supplementary material), and we conclude that our 2D relief model is indeed sensitive to range-scale variations in erosion strength. Importantly, our results suggest that the present-day elevation of the Himalayas may result primarily from strong erosion (emplaced) along the eastern margin since ~15 Ma.

3.2. Geodynamic models of India/Eurasia convergence

The plate tectonic implications of our simple analytic model results can be tested explicitly by using global computer simulations of the coupled mantle/lithosphere system (Iaffaldano and Bunge, 2009; Kong and Bird, 1995). These geodynamic simulations have already been applied successfully in earlier studies of the Nazca/South America plate motion history, and elsewhere (Iaffaldano and Bunge, 2009). They solve the momentum balance in the Earth's mantle and the lithosphere, and account explicitly for plate configurations, the global relief of continents and oceans, as well as realistic mantle related driving forces to compute instantaneous global plate velocities (see supplementary material for details). Importantly, our geodynamic modelling approach allows us to test hypotheses of paleo-elevation derived from our simple analytic erosion models directly as a set of tectonic initial and final state scenarios — that is, to compute global plate velocities for conditions of elevation at the peak of monsoon intensification and at present-day. Specifically, we perform two distinct simulations of global plate motions: in one we assume present-day elevation at the global scale, with higher resolution in the Himalayas and Tibetan plateau (Fig. 7A). In our second simulation we adjust elevation in the eastern Himalayan according to the predicted relief from the 2D analytic model (Fig. 7B). Computed global plate velocities are shown in Fig. 8. From this we note that India indeed

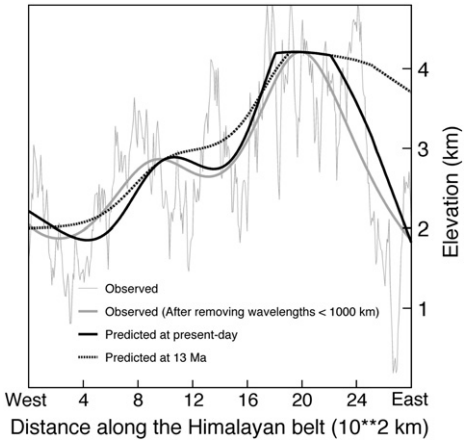

Fig. 6. Prensent-day and past Himalayan elevation as observed and predicted from 2D analytic models. We model relief as the algebraic sum of time- and space-dependent contributions from mountain building and erosion rates, integrated since time of continental collision ~50 Ma (see Section 3.1 in the main text for more details). Grey thin line is the observed elevation at the present-day. At any distance, we report the average value observed along a track cutting into the Himalayas parallel to the direction of India/Eurasia convergence. Thick grey line is the observed elevation after short wavelengths have been filtered out to preserve wavelengths longer that 1000 km. Solid black is the prediction of our model at the present-day. We compare it against the observed elevation, filtered for wavelength shorter than 1000 km (thick grey). Based on the good agreement, we trust our model in its prediction of elevation at 13 Ma (dashed black), when the monsoon had reached its first peak (see Fig. 2). We infer that prior to monsoon intensification, elevation in eastern Himalayas was significantly different from the one at present-day, featuring an average relief as high as 4 km. At the same time, central and western Himalayas are predicted to be very similar to the present-day.

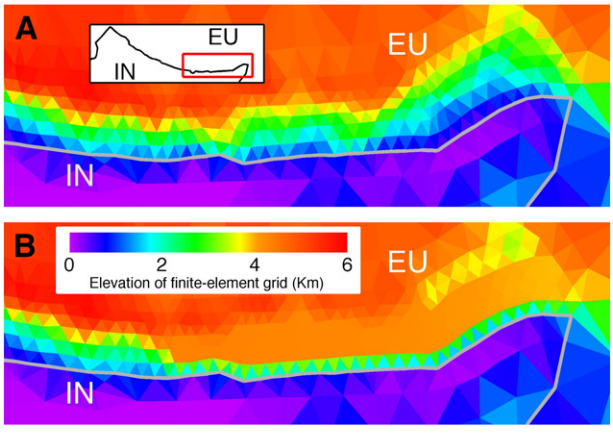

Fig. 7. Elevation in central and eastern Himalayas (red box outlines the region) cast within two finite-element global grids. Plate boundaries are in grey. Grid in (A) employs present-day observed elevation. Grid in (B) features a modified Himalayan elevation, based on the prediction of our 2D relief model at 13 Ma (see Fig. 6). Finite-element elevation elsewhere on the globe is the same in both grids, and equals the present-day observation. The two numerical grids are utilised in two distinct simulations of global coupled mantle/lithosphere dynamics (see Section 3.2 in the main text).

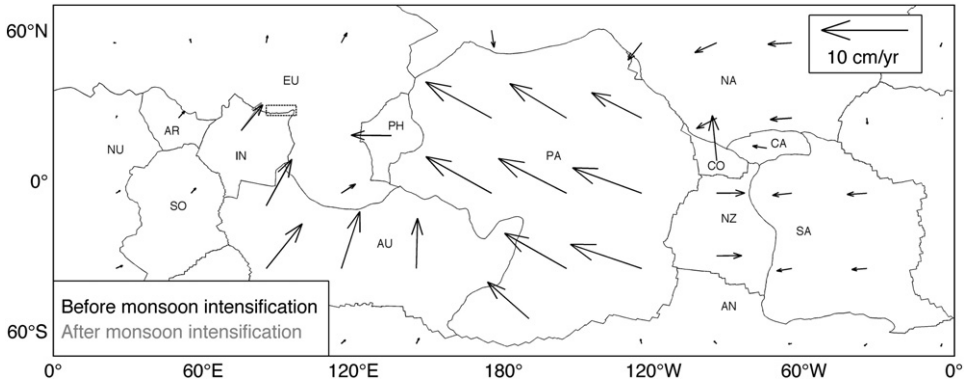

Fig. 8. Predicted global plate motions in the Hotspots reference frame before (black arrows) and after (grey arrows) monsoon intensification — arrows are shown at selected locations. Plate velocities are computed through global finite-element models of the coupled mantle/lithosphere system in two distinct cases: one that casts the present-day elevation within the global finite-element grid, particularly along the central and eastern Himalayas (see Fig. 7A). The other simulation features a modified relief only in the eastern Himalayas (see Fig. 7B) according to our reconstruction of elevation at 13 Ma (see Fig. 6), immediately before the period of intensified monsoon. While a change in the Indian plate (IN) motion is visible, note that predicted velocities of other plates do not change significantly (black arrows overlap to grey ones for all plates other than India). Plate boundaries are in grey. AN — Antarctica, AR — Arabia, CA — Caribbean, CO — Cocos, NA — North America, NU — Nubia, NZ — Nazca, PA — Pacific, PH — Philippine, SA — South America, and SO — Somalia.

undergoes a counter-clockwise rotation after intensification of the monsoon, as its convergence direction rotates westward. Also the dynamics of other plates (magnitude and direction of their velocities) compares well with observations, and no other velocity change results from the assumed erosion of the eastern Himalayas.

We estimate the impact of eroded topography on Indian plate motion as the difference between the two velocity fields (Fig. 9). Our simulations cast India and Australia as two separate plates, according to published observations of the Indian ocean-floor (Bull and Scrutton, 1990; Stein and Okal, 1978). However we also explore a different scenario: one where we assume India and Australia to be merged into a single Indo-Australian plate. When the plates are assumed separated, we predict a velocity change for India of ~8 mm/yr directed trench-normal in the eastern margin, as well as a velocity change of ~5 mm/yr directed trench-parallel in the western margin (Fig. 9 — black arrows). These predictions agree with our reconstruction of India/Eurasia plate motion (Figs. 3–5). More importantly, we verified that the induced velocity change is indeed a rigid body rotation, well described by the Euler pole [64°E 13°N 0.1°/Myr] (Fig. 9 — black dot). We do not find similar results when India and Australia are assumed as a single plate. In this case our simulations predict a minor velocity change for the larger Indo-Australian plate (Fig. 9 — grey arrows), as small as 2 mm/yr. Moreover, the predicted velocity fails to be described by a single Euler pole. Because the relief along eastern Himalayas is the sole varying parameter between the two simulations, our results link the observed rotation of India explicitly to the local release of potential energy along the eastern India/Eurasia plate boundary following intensification of the monsoon. It is worth noting that in a reference frame fixed with the slowly moving Eurasian plate, our models always predict India moving slower than the Australian plate, despite the increased convergence along eastern Himalayas (Fig. 8). Therefore the tectonic regime within the Indian Ocean becomes less compressive since the time of monsoon intensification, and only if India were to move faster than Australia the regime would turn into extensive.

4. Discussion and conclusions

Our results support the notion that faster erosion in the eastern Himalayas locally reduced tectonic resistance against India/Eurasia plate convergence. Specifically, our models indicate that the inferred topography reduction is responsible for a release of 3 to 7 TN/m against Indian convergence. Consequently, Indian plate motion increased by ~8 mm/yr across the eastern margin, and by an almost equal amount along the western margin. This kinematics is equivalently described by a counter-clockwise rigid rotation of India about a pole located north of the Carlsberg ridge, within the Indian plate. In other words, spatial variations of the along-strike relief of the Himalayas appear sufficient to explain the unusual solid body rotation of India in quantitative terms. Our result that such motion is not

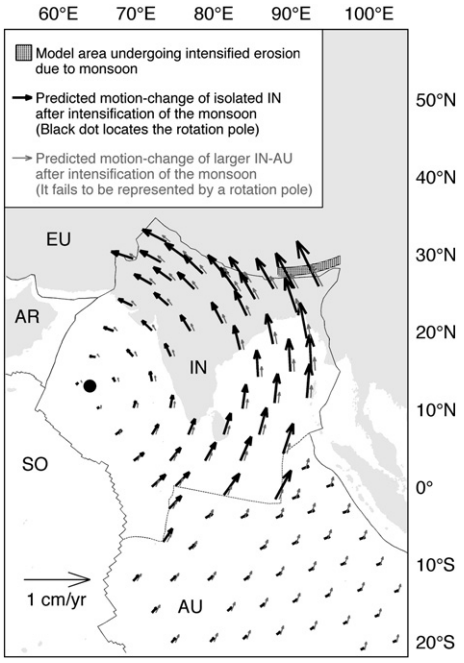

Fig. 9. Indian plate-motion change following erosion of eastern Himalayas due to intensified monsoon. Impact of erosion in eastern Himalayas on Indian plate motion is estimated as the difference between the velocity fields computed before and after (respectively black and grey arrows in Fig. 8) simulated intensification of the monsoon. We predict a velocity change induced on India as high as 8 mm/yr (black arrows), directed normal to the eastern IN/EU margin. An almost equal increase is predicted for the trench-parallel component along the western margin. Numerical result compares well with our reconstruction of India/Eurasia kinematics (see Figs. 3–5). Importantly, predicted change of Indian plate motion is well described by the Euler pole [64°E 12°N 0.1°/Myr] (black dot), within Indian plate itself. We do not find as satisfactory results when we similarly test the effect of erosion in eastern Himalayas on a larger Indo-Australian plate, cast in our finite-element grid by removing the shared boundary in between (dashed black line). In this case in fact we predict on most of the larger Indo-Australian plate velocity changes as small as 2 mm/yr, which fail to be described through a single Euler pole. Our results lend further support to the notion that India was already an independent tectonic unit separate from Australia at the time of monsoon intensification. Oceans are in white, continents in grey. Plate boundaries are in black, plate names as in Fig. 8.

predicted if we assume a single Indo-Australian plate lends independent support to the idea that India must have been a separate tectonic unit prior to monsoon intensification (Wiens et al., 1985). This should be of no surprise: a single Indo-Australian plate would offer a larger basal area for mantle induced shear tractions, in addition to subduction related forcing along the Java–Sumatra trench, plate boundary forces in the southwest Pacific, and forcing related to spreading along the Carlsberg and Indian ridges. Within such a large plate the reduced gravitational potential energy along the eastern Himalayas, which represents only a small portion of the entire boundary of the larger Indo-Australian plate, would therefore more likely be balanced by internal deformation rather than a rigid plate rotation. Furthermore, our inference is compatible with the timing of break-up implied by earlier studies. Cloetingh and Wortel (1985, 1986) noted that the Indo-Australian plate was subject to southward resistance arising from the gravitational potential of the larger Tibetan plateau, combined with northward pull from the young lithosphere subducting beneath Java/Sumatra. The pattern implied by these boundary forces resulted in an unusually high level of stresses in the lithosphere, evident from local deformation (Geller et al., 1983) and seismicity (Stein et al., 1987) within the Bay of Bengal. The significant gradients of age, and therefore of thickness of the Indio-Australian plate possibly acted as a guide to focus stresses within in the Indian Ocean, thus triggering the break-up. Reconstructions of past ocean floor age (Mueller et al., 2008) indicate that these conditions were certainly in place prior to monsoon intensification.

Our results therefore reveal that lateral variations in plate-coupling may arise as a consequence of climate phenomena, and that such variations may be detectable in the plate motion record. Since climate is in turn often affected by geologic processes at plate margins, such as mountain building, our results imply continuous feedback mechanisms between climate dynamics and plate motions, where at times one controls the others and *vice-versa*. Plate coupling forces therefore should not be regarded as steady boundary conditions across orogenic belts. Rather they might undergo variations related, among others, to climate-controlled morphological processes. In the search for relationships between climate and surface morphology, this represents the natural evolution of dynamic models that currently implement velocity rather than stress as boundary condition (e.g. Whipple and Meade, 2006; Willett, 1999). The strong dependence of convergence rates from the force balance at plate boundaries suggests that dynamic rather than kinematic conditions should be used in numerical models.

Two more implications are worth noting. Spreading along mid ocean ridges is often regarded as a process where rate, geometry and degree of asymmetry are determined, at least in part, by local ridge-mantle interactions (Mueller et al., 1998). Our results, however, link the recent spreading history along the Carlsberg ridge directly to variations of the tectonic regime at a distant convergent margin. In fact the rotation of India predicted from our geodynamic models fits reasonably well the peculiar eastward shift of the India/Somalia Euler pole after monsoon intensification (Fig. 10 — black squares). Specifically, we add the monsoon-induced Indian rotation (Fig. 10 — black dot) to the India/Somalia observed Euler pole for the stage from 3An.2o to 2An.3o, to obtain a prediction of the India/Somalia Euler pole for the stage from 2An.3o to the present-day (Fig. 10 — white triangle). The resulting Euler pole is [35°E 22°N 0.45°/Myr] and compares well with the observed one for the same stage [34°E 20°N 0.44°/Myr].

A second implication concerns the location of Euler poles. Commonly the relative motion of plate pairs is described by an Euler pole located far away from the plate boundary they share, as far away as ~90°, resulting in mostly translational relative motion between the plates on the globe. It has been shown that plate pairs sharing a diffuse boundary – that is, a deformation zone usually hundreds to thousands of kilometres wide – tend to locate their Euler pole within their wide boundary (Gordon, 1998), a feature that has been linked to geometrical effects minimising the net torque along the shared boundary (Zatman et al., 2001). However, our findings suggest an additional cause for rigid rotation, namely lateral variations in plate-boundary forces. In other words, plate boundary forces should be regarded as capable to modify the force balance of two adjacent plates sufficiently to generate a rotational component with an Euler pole located in the vicinity of, or within, both plates even when they share a narrow margin.

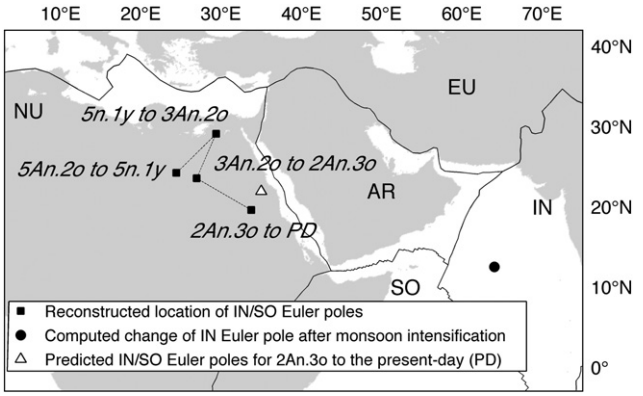

Fig. 10. Predicted and observed eastward shift of the India/Somalia Euler pole. We add the rotation of India predicted from our models (black dot) to the observed India/Somalia Euler pole for the stage 3An.2o to 2An.3o, to arrive at a prediction of the India/Somalia pole location for the stage 2An.30 to present-day (white triangle). The resulting Euler pole is [35°E 22°N 0.45°/Myr], and compares well with the observed one for the same stage [34°E 20°N 0.44°/Myr]. Oceans are in white, continents in grey. Plate boundaries are in black, plate names as in Fig. 8.

Acknowledgments

We thank J.-P. Avouac, S. Cande, P. Molnar, and E. Rohling for providing useful feedbacks. We thank an anonymous reviewer for careful comments. G.I. acknowledges support from the Reginald A. Daly Postdoctoral Fellowship at Harvard University and the Ringwood Fellowship at the Australian National University. L.H. acknowledges S. Bonnet, D. Lague, and P. Davy for stimulating discussions.

Appendix A. Supplementary data

Supplementary data to this article can be found online at doi:10.1016/j.epsl.2011.02.026.

References

An, Z., Kutzbach, J.E., Prell, W.L., Porter, S.C., 2001. Evolution of Asian monsoons and phased uplift of the Himalaya–Tibetan plateau since late Miocene times. Nature 411, 62–66.

Avouac, J.-P., Burov, E.B., 1996. Erosion as a driving mechanism of intercontinental mountain growth. J. Geophys. Res. 101, 17747–17769.

Beaumont, C., Fullsack, P., Hamilton, J., 1992. Erosional control of active compressional orogens. In: McClay, K.R. (Ed.), Thrust Tectonics. Chapman and Hall, pp. 1–18.

Bonini, M., Corti, G., Innocenti, F., Manetti, P., Mazzarini, F., Abebe, T., Pecskay, Z., 2005. Evolution of the Main Ethiopian Rift in the frame of Afar and Kenya rifts propagation. Tectonics 24, C1007.

Boos, W.R., Kuang, Z., 2010. Dominant control of the South Asian monsoon by orographic insulation versus plateau heating. Nature 463, 218–222.

Bull, J.M., Scrutton, R.A., 1990. Fault reactivation in the central Indian Ocean and the rheology of oceanic lithosphere. Nature 344, 855–858.

Bunge, H.-P., Richards, M.A., Lithgow-Bertelloni, C., Baumgardner, J.R., Grand, S.P., Romanovicz, B.A., 1998. Time scales and heterogeneous structures in geodynamic earth models. Science 280, 91–95.

Burbank, D.W., Blythe, A.E., Putkonen, J., Pratt-Sitaula, B., Gabet, E., Oskin, M., Barros, A., Ojha, T.P., 2003. Decoupling of erosion and precipitation in the Himalayas. Nature 426, 652–655.

Burg, J.P., Nievergelt, P., Oberli, F., Seward, D., Davy, P., Maurin, J.C., Diao, Z., Meier, M., 1998. The Namche Barwa syntaxis: evidence for exhumation related to compressional crustal folding. J. Asian Earth Sci. 16, 239–252.
Chemenda, A.I., Burg, J.-P., Mattauer, M., 2000. Evolutionary model of the Himalaya–Tibet system: geopoem based on new modelling, geological and geophysical data. Earth Planet. Sci. Lett. 174, 397–409.
Clift, P.D., Hodges, K.V., Heslop, D., Hannigan, R., van Long, H., Calves, G., 2008. Correlation of Himalayan exhumation rates and Asian monsoon intensity. Nat. Geosci. 1, 875–880.
Cloetingh, S., Wortel, R., 1985. Regional stress field of the Indian plate. Geophys. Res. Lett. 12, 77–80.
Cloetingh, S., Wortel, R., 1986. Stress in the Indo-Australian plate. Tectonophysics 132, 49–67.
Conder, J.A., Forsyth, D.W., 2001. Seafloor spreading on the southeast Indian ridge over the last one million years: a test of the Capricorn plate hypothesis. Earth Planet. Sci. Lett. 188, 91–105.
Copley, A., Avouac, J.-P., Royer, J.-Y., 2010. India-Asia collision and the Cenozoic slow down of the Indian plate: implications for the forces driving plate motions. J. Geophys. Res. 115, B03410.
DeMets, C., Gordon, R.G., Royer, J.-Y., 2005. Motion between the Indian, Capricorn and Somalian plates since 20 Ma: implications for the timing and magnitude of distributed lithospheric deformation in the equatorial Indian Ocean. Geophys. J. Int. 161, 445–468.
Finlayson, D.P., Montgomery, D.R., Hallet, B., 2002. Spatial coincidence of rapid inferred erosion with young metamorphic massifs in the Himalayas. Geology 3, 219–222.
Forte, A.M., Moucha, R., Rowley, D.B., Quere, S., Mitrovica, J.X., Simmons, N.A., Grand, S.P., 2009. Recent tectonic plate decelerations driven by mantle convection. Geophys. Res. Lett. 36, L23301.
Galy, A., France-Lanord, C., 2001. Higher erosion rates in the Himalaya: geochemical constraints on riverine fluxes. Geology 29, 23–26.
Garzione, C.N., DeCelles, P.G., Hodkinson, D.G., Ojha, T.P., Upreti, B.N., 2003. East-west extension and Miocene environmental change in the southern Tibetan plateau: Thakkhola graben, central Nepal. Geol. Soc. Am. Bull. 115, 3–20.
Geller, C.A., Weissel, J.K., Anderson, R.N., 1983. Heat transfer and intraplate deformation in the central Indian Ocean. J. Geophys. Res. 88, 1018–1032.
Ghosh, A., Holt, W.E., Flesch, L.M., Haines, A.J., 2006. Gravitational potential energy of the Tibetan Plateau and the forces driving the Indian plate. Geology 34, 321–324.
Gordon, R.G., 1998. The plate tectonic approximation: plate non-rigidity, diffuse plate boundaries, and global plate reconstructions. Annu. Rev. Earth Planet. Sci. 26, 615–642.
Gordon, R.G., DeMets, C., Royer, J.-Y., 1998. Evidence for long-term diffuse deformation of the lithosphere of the equatorial Indian Ocean. Nature 395, 370–374.
Gordon, R.G., Argus, D.F., Royer, J.-Y., 2008. Space geodetic test of kinematic models for the Indo-Australian composite plate. Geology 36, 827–830.
Horner-Johnson, B.C., Gordon, R.G., Argus, D.F., 2007. Plate kinematic evidence for the existence of a distinct plate between the Nubian and Somalian plates along the Southwest Indian Ridge. J. Geophys. Res. 112, B05418.
Husson, L., Ricard, Y., 2004. Stress balance above subduction: application to the Andes. Earth Planet. Sci. Lett. 222, 1037–1050.
Husson, L., Conrad, C.P., Faccenna, C., 2008. Tethyan closure, Andean orogeny, and westward drift of the Pacific basin. Earth Planet. Sci. Lett. 271, 303–310.
Iaffaldano, G., Bunge, H.-P., 2009. Relating rapid plate motion variations to plate boundary forces in global coupled models of the mantle/lithosphere system: effects of topography and friction. Tectonophysics 474, 393–404.
Iaffaldano, G., Bunge, H.-P., Dixon, T.H., 2006. Feedback between mountain belt growth and plate convergence. Geology 34, 893–896.
Iaffaldano, G., Bunge, H.-P., Buecker, M., 2007. Mountain belt growth inferred from histories of past plate convergence: a new tectonic inverse problem. Earth Planet. Sci. Lett. 260, 516–523.
Klitgord, K.D., Schouten, H., 1986. Plate kinematics of the central Atlantic. In: Vogt, P.R., Tucholke, B.E. (Eds.), The Geology of North America. Geol. Soc. of Am, Boulder, Colorado, pp. 351–378.
Kong, X., Bird, P., 1995. Shells: a thin-shell program for modeling neotectonics of regional or global lithosphere with faults. J. Geophys. Res. 100, 22129–22131.
Le Treut, H., Li, Z.X., Forrichon, M., 1994. Sensitivity of the LMD general circulation model to greenhouse forcing associated with two different cloud water parameterizations. J. Climatol. 7, 1827–1841.
Lemaux, J., Gordon, R.G., Royer, J.-Y., 2002. Location of the Nubia–Somalia boundary along the Southwest Indian Ridge. Geology 30, 339–342.
Lourens, L., Hilgen, F.J., Laskar, J., Shackleton, N.J., Wilson, D., 2004. The Neogene Period. In: Gradstein, F., Ogg, J., Smith, A. (Eds.), A Geologic Time Scale. Cambridge University Press, London, pp. 409–440.
McQuarrie, N., Stock, J.M., Verdel, C., Wernicke, B.P., 2003. Cenozoic evolution of Neotethys and implications for the causes of plate motions. Geophys. Res. Lett. 30, 2036.
Meade, B.J., Conrad, C.P., 2008. Andean growth and the deceleration of South American subduction: time evolution of a coupled orogen-subduction system. Earth Planet. Sci. Lett. 275, 93–101.
Merkouriev, S., DeMets, C., 2006. Constraints on Indian plate motion since 20 Ma from dense Russian magnetic data: implications for Indian plate dynamics. Geochem. Geophys. Geosyst. 7, Q02002.
Merkouriev, S., DeMets, C., 2008. A high-resolution model for Eurasia–North America plate kinematics since 20 Ma. Geophys. J. Int. 173, 1064–1083.
Molnar, P., Stock, J.M., 2009. Slowing India's convergence with Eurasia since 20 ma and its implications for Tibetan mantle dynamics. Tectonics 28, 357–396.
Molnar, P., England, P., Martinod, J., 1993. Mantle dynamics, uplift of the Tibetan plateau, and the Indian monsoon. Rev. Geophys. 31, 357–396.
Montgomery, D.R., Brandon, M.T., 2002. Topographic controls on erosion rates in tectonically active mountain ranges. Earth Planet. Sci. Lett. 201, 481–489.
Mueller, R.D., Roest, W.R., Royer, J.-Y., 1998. Asymmetric sea-floor spreading caused by ridge-plume interactions. Nature 396, 455–459.
Mueller, R.D., Royer, J.-Y., Cande, S.C., Roest, W.R., Maschenkov, S., 1999. New constraints of the Carribean plate tectonic evolution. In: Mann, P. (Ed.), Sedimentary Basins of the World, vol. 4. Elsevier, pp. 33–59.
Mueller, R.D., Sdrolias, M., Gaina, C., Steinberger, B., Heine, C., 2008. Long-term sea-level fluctuations driven by ocean basin dynamics. Science 319, 1357–1362.
Patriat, P., Achache, J., 1984. India–Eurasia collision chronology has implications for crustal shortening and driving mechanism of plates. Nature 311, 615–621.
Patriat, P., Sloan, H., Sauter, D., 2008. From slow to ultraslow: a previously undetected event at the Southwest Indian Ridge at ca. 24 Ma. Geology 36, 207–210.
Pidwirny, M., 2006. Global Distribution of Precipitation, Fundamentals of Physical Geography, 2nd edition.
Pik, R., Marty, B., Carignan, J., Yirgu, G., Ayalew, T., 2008. Timing of East African Rift development in southern Ethiopia: implication for mantle plume activity and evolution of topography. Geology 36, 167–170.
Ramstein, G., Fluteau, F., Besse, J., Joussaume, S., 1997. Effect of orogeny, plate motion and land-sea distribution on Eurasian climate change over the past 30 million years. Nature 386, 789–795.
Royer, J.-Y., Gordon, R.G., 1997. The motion and boundary between the Capricorn and Australian plates. Science 277, 1268–1274.
Royer, J.-Y., Gordon, R.G., Horner-Johnson, B.C., 2006. Motion of Nubia relative to Antarctica since 11 Ma: implications for Nubia–Somalia, Pacific–North America, and India–Eurasia motion. Geology 34, 501–504.
Srivastava, S.P., Tapscott, C.R., 1986. Plate kinematics of the North Atlantic. In: Vogt, P.R., Tucholke, B.E. (Eds.), The Geology of North America. Geol. Soc. of Am, Boulder, Colorado, pp. 379–404.
Srivastava, S.P., Roest, W.R., Kovacs, L.C., Oakey, G., Levesque, S., Verhoef, J., Macnab, R., 1990. Motion of Iberia since the Late Jurassic; results from detailed aeromagnetic measurements in the Newfoundland Basin. Tectonophysics 184, 229–260.
Stamps, D.S., Calais, E., Saria, E., Hartnady, C., Nocquet, J.-M., Ebinger, C.J., Fernandes, R.M., 2008. A kinematic model for the East African Rift. Geophys. Res. Lett. 35, L05304.
Stein, S., Okal, E.A., 1978. Seismicity and tectonics of the Ninetyeast ridge area: evidence for internal deformation of the Indian plate. J. Geophys. Res. 83, 2233–2245.
Stein, S., Cloetingh, S., Wiens, D.A., Wortel, R., 1987. Why does near ridge extensional seismicity occur primarily in the Indian Ocean? Earth Planet. Sci. Lett. 82, 107–113.
Summerfield, M.A., Hulton, N.J., 1994. Natural controls of fluvial denudation rates in major world drainage basins. J. Geophys. Res. 99, 13871–13883.
Tapponnier, P., Zhiqin, X.Z., Roger, F., Meyer, B., Arnaud, N., Wittlinger, G., Jingsui, Y., 2001. Oblique stepwise rise and growth of the Tibet plateau. Science 294, 1671–1677.
Thiede, R.C., Bookhagen, B., Arrowsmith, J.R., Sobel, E.R., Strecker, M.R., 2004. Climatic control on rapid exhumation along the Southern Himalayan Front. Earth Planet. Sci. Lett. 222, 791–806.
Torsvik, T.H., Steinberger, B., Gurnis, M., Gaina, C., 2010. Plate tectonics and the net lithosphere rotation over the past 150 My. Earth Planet. Sci. Lett. 291, 106–112.
Travese, A., 1982. A Response of World Vegetation to Neogene Tectonic and Climatic Events. Alcheringa.
Whipple, K.X., Meade, B.J., 2006. Orogen response to changes in climatic and tectonic forcing. Earth Planet. Sci. Lett. 243, 218–228.
Wiens, D.A., DeMets, C., Gordon, R.G., Stein, S., Argus, D., Engeln, J.F., Lundgren, P., Quible, D., Stein, C., Weinstein, S., Woods, D.H., 1985. A diffuse plate boundary model for Indian Ocean tectonics. Geophys. Res. Lett. 12, 429–432.
Willett, S.D., 1999. Orogeny and orography: the effects of erosion on the structure of mountain belts. J. Geophys. Res. 104, 28957.
Wolfe, J.A., 1985. The carbon cycle of atmospheric CO2: Natural variations Archean to present, in: Sunquist, E.T., Broecker, W.S. (Eds.), pp. 357–375.
Zatman, S., Gordon, R.G., Richards, M.A., 2001. Analytic models for the dynamics of diffuse oceanic plate boundaries. Geophys. J. Int. 145, 145–156.